Mechanistic Characterization of *N*-Formimino-L-glutamate Iminohydrolase from *Pseudomonas aeruginosa*[†]

Ricardo Martí-Arbona and Frank M. Raushel*

Department of Chemistry, P.O. Box 30012, Texas A&M University, College Station, Texas 77842-3012

Received August 16, 2006; Revised Manuscript Received September 27, 2006

ABSTRACT: *N*-Formimino-L-glutamate iminohydrolase (HutF) from *Pseudomonas aeruginosa* catalyzes the deimination of *N*-formimino-L-glutamate in the histidine degradation pathway. An amino acid sequence alignment between HutF and members of the amidohydrolase superfamily containing mononuclear metal centers indicated that residues Glu-235, His-269, and Asp-320 are involved in substrate binding and activation of the nucleophilic water molecule. The purified enzyme contained up to one equivalent of zinc. The metal was removed by dialysis against the metal chelator dipicolinate with the complete loss of catalytic activity. Enzymatic activity was restored by incubation of the apoprotein with Zn^{2+}, Cd^{2+}, Ni^{2+}, or Cu^{2+}. The mutation of Glu-235, His-269, or Asp-320 resulted in the diminution of catalytic activity by two to six orders of magnitude. Bell-shaped profiles were observed for k_{cat} and k_{cat}/K_m as a function of pH. The pK_a of the group that must be unprotonated for catalytic activity was consistent with the ionization of His-269. This residue is proposed to function as a general base in the abstraction of a proton from the metal-bound water molecule. In the proposed catalytic mechanism, the reaction is initiated by the abstraction of a proton from the metal-bound water molecule by the side chain imidazole of His-269 to generate a tetrahedral intermediate of the substrate. The collapse of the tetrahedral intermediate commences with the abstraction of a second proton via the side chain carboxylate of Asp-320. The C−N bond of the substrate is subsequently cleaved with proton transfer from His-269 to form ammonia and the *N*-formyl product. The postulated role of the invariant Glu-235 is to ion pair with the positively charged formimino group of the substrate.

N-Formimino-L-glutamate iminohydrolase (HutF) catalyzes the formation of ammonia and *N*-formyl-L-glutamate from *N*-formimino-L-glutamate (**1**) as shown in Scheme 1. This reaction sequence is the penultimate step in one of the three known pathways for the degradation of L-histidine to L-glutamate (*1*). In one of the bacterial catabolic pathways, L-histidine is initially converted to urocanate and ammonia by histidine ammonia-lyase (HutH[1]). Urocanase (HutU) then transforms urocanate to L-5-imidazolone-4-propionate, which is subsequently hydrolyzed to *N*-formimino-L-glutamate by imidazolone propionate amidohydrolase (HutI). HutF catalyzes the formation of *N*-formyl-L-glutamate, which is then hydrolyzed by HutG to generate formate and L-glutamate. In *Pseudomonas aeruginosa* we have demonstrated that Pa5106 (gi: 15600299) is HutF and that Pa5091 is HutG (*2*). *P. aeruginosa* can also hydrolyze *N*-formimino-L-glutamate directly to L-glutamate and formamide by the action of Pa3175 (*2*).

Scheme 1
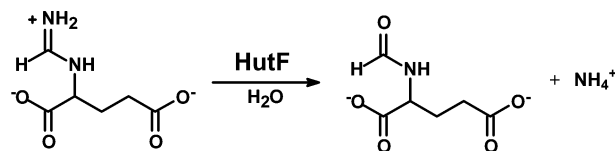
HutF has been identified as a member of the amidohydrolase superfamily (AHS). This superfamily was first recognized from the three-dimensional structural similarities found within the active sites and protein folds of urease (URE), phosphotriesterase (PTE), and adenosine deaminase (ADA) (*3*). Members of this functionally diverse superfamily are found in every organism sequenced to date (*4, 5*) and are characterized by a mono- or binuclear metal center embedded within the *C*-terminal end of a $(\beta/\alpha)_8$ barrel structural fold (*3*). HutF most closely resembles the sequences possessed by enzymes that catalyze the deamination of the heterocyclic base, cytosine (*2*), and the herbicide, atrazine (*3*). The structural similarity within these three substrates is shown in Scheme 2.

Relatively little is known about the reaction mechanism for the deimination of *N*-formimino-L-glutamate by HutF. Based upon the sequence alignment of HutF with the two most closely structurally characterized analogues, it is anticipated that this enzyme will possess a mononuclear metal center in the active site. The single divalent cation will be ligated to His-56 and His-58 from the end of β-strand

¹ Abbreviations: HutH, histidine ammonia lyase; HutU, urocanase; HutI, imidazolone propionate amidohydrolase; HutF, *N*-formimino-L-glutamate deiminase; HutG, *N*-formyl-L-glutamate amidohydrolase; HEPES, *N*-2-hydroxyethylpiperazine-*N*′-2-ethanesulfonic acid; PMSF, phenylmethylsulfonyl fluoride; IPTG, isopropyl-thiogalactoside; CDA, cytosine deaminase; ADA, adenosine deaminase.

Scheme 2
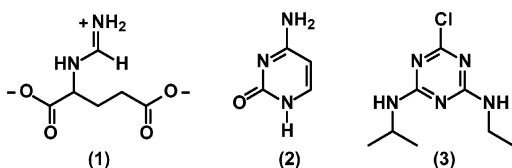
1, His-232 from β-strand 5, and Asp-320 from β-strand 8. A water molecule will function as the fifth ligand to the lone divalent cation. This water molecule will be hydrogen bonded to His-269 from the end of strand 6 and to the carboxylate of Asp-320 that also interacts with the divalent cation. The remaining invariant residue within the active site of HutF is Glu-235. This residue is located at the end of strand 5 within an HxxE motif that is found in members of the AHS that catalyze the deamination of aromatic bases such as adenosine, guanine, and cytosine. The purported function of the analogous residue in adenosine and cytosine deaminase is for proton donation to the aromatic base upon nucleophilic attack by water. A homology model for the active site of HutF based upon these considerations is presented in Figure 1.

The current investigation presents the biochemical characterization of the mechanism of reaction of HutF from *P. aeruginosa*. This reaction mechanism was probed to enhance our current understanding of the breadth of the reactions catalyzed by members of the amidohydrolase superfamily. The active site core of HutF most closely resembles those enzymes that catalyze a nucleophilic aromatic substitution. How these highly conserved residues are marshaled together within the active site of HutF to catalyze the deimination of an *N*-formimino group will aid in our attempt to correctly annotate enzymes of unknown function within this diverse superfamily of enzymes. The functional roles of those residues anticipated to be directly involved in catalysis and substrate specificity were addressed by the construction and characterization of site-directed mutant enzymes. The proton-transfer steps in the catalytic transformation were probed by the measurement of the kinetic constants as a function of pH. The role of the active site metal was interrogated by formation and reconstitution of apo-HutF with a variety of divalent cations.

MATERIALS AND METHODS

Materials. All chemicals were obtained from Sigma-Aldrich, unless otherwise stated. The genomic DNA from *P. aeruginosa* was purchased from the American Type Culture Collection (ATCC). The oligonucleotide synthesis and DNA sequencing reactions were performed by the Gene Technology Laboratory of Texas A&M University. The pET30a(+) expression vector and the BL21(DE3)star cells were acquired from Novagen. The Quick Change site-directed mutagenesis kit was purchased from Stratagene.

Cloning and Site Directed Mutagenesis. The gene encoding for Pa5106 (HutF) was cloned from *P. aeruginosa* PA01 into a pET30a(+) expression vector as previously described (*2*). Site directed mutagenesis of HutF at residues Glu-235, His-269, and Asp-320 was accomplished using the Quick Change site directed mutagenesis kit. The wild-type and mutant forms of HutF were expressed in BL21(DE3)star cells.
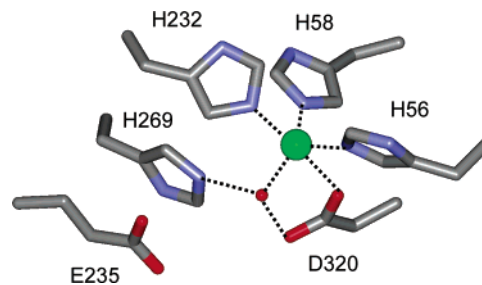
FIGURE 1: Homology model for the active site of HutF. The model was generated from a sequence alignment of HutF with cytosine deaminase from *E. coli*. The coordinates for cytosine deaminase were obtained from PDB code 1k6w (*9*).

Purification of Wild-Type and Mutant HutF. A single colony was grown overnight in 50 mL of LB medium containing 50 μM kanamycin and was used to inoculate 4 L of the same medium. Cell cultures were grown at 37 °C with a rotatory shaker until an A_{600nm} of ∼0.6 was reached, after which induction was initiated by the addition of 1.0 mM isopropyl-thiogalactoside (IPTG). The culture was incubated overnight at 30 °C and the bacterial cells were isolated by centrifugation at 6500*g* for 15 min at 4 °C. The pellet was resuspended in 50 mM HEPES buffer at pH 7.5 (buffer A) containing 0.1 mg/mL of the protease inhibitor phenylm-ethylsulfonyl fluoride (PMSF) per gram of cells and disrupted by sonication. The soluble protein was separated from the cell debris by centrifugation at 12000*g* for 15 min at 4 °C. Nucleic acids were precipitated by the addition of protamine sulfate to a 1.5% (w/v) solution. The protein solution was fractionated between 40% and 60% saturated ammonium sulfate. The precipitated protein from the 40−60% saturated ammonium sulfate solution was resuspended in buffer A and loaded onto a High Load 26/60 Superdex 200 prep grade gel filtration column (GE Health Care) and eluted with buffer A. Fractions containing the *N*-formimino-L-glutamate de-iminase activity were pooled and loaded onto a 6 mL Resource Q anion exchange column (GE Health Care) and eluted with a gradient of NaCl in 20 mM HEPES at pH 7.5 (buffer B). The fractions that contained HutF were pooled and reprecipitated with a 65% saturated ammonium sulfate solution, centrifuged at 12000*g* for 15 min at 4 °C, and resuspended in a minimal amount of buffer A. The final step in the purification scheme was accomplished with a High Load 26/60 Superdex 200 prep grade gel filtration column where the protein was eluted with buffer A. The purity of the protein during the isolation procedure was monitored by SDS−PAGE.

The purification of HutF mutants was performed as described above for the wild-type HutF with some modifications. These amendments included the induction of protein expression using 500 μM IPTG and growing the cells at 20 °C. The nucleic acids were hydrolyzed by the addition of 5 U/mL of Benzonase for 1 h. The protein solution was fractionated between 30% and 65% saturated ammonium sulfate. The remaining purification steps were unchanged.

Specific Activity Determination. The specific activity of HutF toward the deimination of *N*-formimino-L-glutamate was followed by coupling the production of ammonia to the oxidation of NADH. The decrease in the concentration of NADH was followed spectrophotometrically at 340 nm using

Table 1: Kinetic Parameters for Metal-Reconstituted HutF and Active Site Mutants[a]

HutF (M)	M^{2+}/subunit	K_m (mM)	k_{cat} (s^{-1})	k_{cat}/K_m (M^{-1}s^{-1})
WT (Zn)	1.2	0.22 ± 0.03	13.2 ± 0.4	(6.0 ± 0.1) × 10^4
WT (Ni)	0.81	2.7 ± 0.1	21.3 ± 0.3	(8.0 ± 0.3) × 10^3
WT (Cd)	1.2	2.1 ± 0.3	31.0 ± 0.1	(1.5 ± 0.2) × 10^4
WT (Cu)	1.7	1.2 ± 0.1	8.5 ± 0.1	(7.3 ± 0.4) × 10^3
E235A (Zn)	0.62	2.2 ± 0.1	(1.0 ± 0.2) × 10^{-1}	(4.7 ± 0.6) × 10^1
E235D (Zn)	0.51	0.66 ± 0.05	(5.0 ± 0.1) × 10^{-3}	7.9 ± 0.6
E235Q (Zn)	0.77	19 ± 2	(1.2 ± 0.1) × 10^{-1}	6.3 ± 0.8
H269A (Zn)	0.12			(1.6 ± 0.1) × 10^{-1}
H269C (Zn)	0.95			(7.3 ± 0.1) × 10^{-1}
H269N (Zn)	0.17			(1.8 ± 0.1) × 10^{-1}
D320A (Zn)	0.50			<2.0 × 10^{-2}
D320C (Zn)	1.0			<2.0 × 10^{-2}

[a] The kinetic parameters were determined with *N*-formimino-L-glutamate as the substrate at pH 8.0, 30 °C, from a fit of the data to eq 1.

a SPECTRAmax-340 microplate reader (Molecular Devices Inc.). The standard assay was modified from that reported by Muszbek et al. (*6*) and contained 100 mM HEPES, pH 7.5, 100 mM KCl, 7.4 mM α-ketoglutarate, 0.4 mM NADH, 6 units of glutamate dehydrogenase, 20 nM of HutF, and *N*-formimino-L-glutamate in a final volume of 250 μL at 30 °C.

Metal Analysis. Metal-free HutF (apo-HutF) was prepared and reconstituted with different divalent metal cations, as previously described (*2*). Purified HutF was treated with 3 mM dipicolinate, pH 5.6, at 4 °C for 48 h. The chelator was removed by loading the protein/chelator mixture onto a PD10 column (GE Health Care) and eluting with metal-free buffer A. The apo-HutF was reconstituted with 1.0 equiv of the desired divalent metal (Zn^{2+}, Co^{2+}, Ni^{2+}, Cd^{2+}, and Mn^{2+}) in 50 mM HEPES at pH 7.5. The metal content of the apo-HutF and reconstituted enzymes was verified using a Perkin-Elmer AAnalyst 700 atomic absorption spectrometer and inductively coupled plasma emission-mass spectrometry (ICP-MS).

pH−Rate Profiles. The pH dependence of the kinetic parameters was determined for the Zn, Cd, Cu, and Ni forms of the wild-type HutF using *N*-formimino-L-glutamate as the substrate. The pH−rate profiles were also obtained for the Zn-substituted forms of the E235Q and E235A mutants. The pH range for the enzymatic assays was between 6.1 and 9.5 in 0.2 pH unit increments. The buffers MES (pH 6.1 and 6.5), PIPES (pH 6.7 to 7.3), HEPES (pH 7.3 to 8.3), TAPS (pH 8.3 to 8.9), and CHES (8.9 and 9.5) were used at a concentration of 100 mM. The pH was measured after completion of the assay.

Data Analysis. The kinetic parameters, k_{cat} and k_{cat}/K_m, were determined by fitting the initial velocity data to eq 1 (*7*), where v is the initial velocity, E_t is the enzyme concentration, k_{cat} is the turnover number, A is the substrate concentration, and K_m is the Michaelis constant. The pH−rate profiles were fit to eq 2 when the value of y (k_{cat} or k_{cat}/K_m) decreases at low and high pH. In this equation c is the pH independent value of y, K_a and K_b are the dissociation constants of the ionizable groups, and H is the hydrogen ion concentration. The pH−rate profiles were fit to eq 3 or 4 when the ionization of two groups with similar ionization constants was determined at either high or low pH, respectively.

$$v/E_t = k_{cat}A/(K_m + A) \qquad (1)$$

$$\log y = \log(c/(1 + (H/K_a) + (K_b/H))) \qquad (2)$$

$$\log y = \log(c/(1 + (H/K_a) + (K_b/H) + ((K_b)^2/(H^2)))) \qquad (3)$$

$$\log y = \log(c/(1 + (H/K_a) + (K_b/H) + (H^2/(K_a)^2))) \qquad (4)$$

RESULTS

Metal Substituted Variants of HutF. The functional significance of a divalent cation in the reaction catalyzed by HutF was probed by formation of the apoenzyme and reconstitution of this protein with a variety of other metal ions. The isolated recombinant protein expressed in *Escherichia coli* was found to contain 0.5 equiv of Zn^{2+} per enzyme subunit and a specific activity of 5.2 s^{-1}. Incubation of HutF with the metal chelator dipicolinate for 3 h at pH 5.6 was effective in the removal of zinc from the active site. A metal analysis of the apoenzyme found 0.03 equiv of zinc per subunit and a specific activity of less than 0.1 s^{-1}. More than 98% of the original catalytic activity was lost after removal of the zinc from the enzyme.

The metal center was reconstituted in about 10 min after the addition of 1 equiv of Cd^{2+}, Cu^{2+}, Ni^{2+}, or Zn^{2+} to the apoenzyme. The reconstitution of apo-HutF with these metal ions resulted in catalytically active enzyme with Cd^{2+} > Ni^{2+} > Zn^{2+} > Cu^{2+} with respect to k_{cat}. The reconstitution of apo-HutF with Co^{2+} and Mn^{2+} could not be accomplished even after 48 h of incubation with up to 10 equiv of metal per subunit of protein. The average metal content per subunit of the reconstituted proteins was 1.2, 0.8, 1.2, and 1.7 for the Zn-, Ni-, Cd-, and Cu-substituted forms of HutF, respectively. The kinetic parameters for the metal-reconstituted variants of HutF are presented in Table 1.

Site-Directed Mutagenesis. Sequence alignments of HutF with the structurally characterized members of the amidohydrolase superfamily indicate that this enzyme is most closely related to those proteins that catalyze the deamination of exocyclic amino groups from nitrogen heterocyclic substrates (*2*). The X-ray crystal structures of adenosine deaminase (*8*) and cytosine deaminase (*9*), in conjunction with these sequence alignments, suggest critical roles for Glu-235, His-269, and Asp-320 in the catalytic activity of HutF. The functional significance of His-269 and Asp-320 in the active site of HutF was assessed by mutation of these residues to alanine, asparagine, and cysteine. The role of Glu-235 was
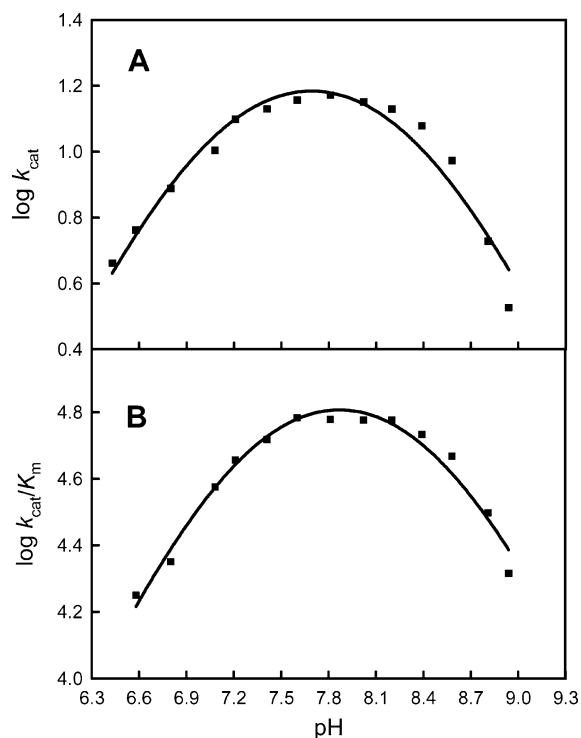
FIGURE 2: pH−rate profiles of k_{cat} and k_{cat}/K_m for the zinc substituted form of HutF. The data were fit to eq 2. Additional details are provided in the text.

FIGURE 3: pH−rate profiles for the metal-reconstituted forms of the wild-type HutF: Cd (○), Ni (●), and Cu (▲). The data for the Ni- and Cu-HutF were fit to eq 2. The pH−rate profile of the Cd-HutF was fit to eq 2 for the variation of k_{cat} with pH and to eq 3 for the variation of k_{cat}/K_m with pH. Additional details are provided in the text and in Table 2.

addressed by mutation to alanine, aspartate, and glutamine. The mutant proteins were purified to homogeneity, and the zinc content of the purified proteins varied from 0.17 to 1.0 equiv of Zn^{2+} per protein subunit. The effects of these mutations on the kinetic parameters of HutF are presented in Table 1.

There was a substantial drop in the catalytic activity as a result of the mutations at each of the three residues. For the three characterized mutations at His-269 the catalytic activity is approximately 5 orders of magnitude lower than that of the wild type enzyme. The values of k_{cat} for these mutants could not be determined since the velocity of the catalyzed reaction was not saturated at the highest concentration of substrate (10 mM). The metal content of the H269A and H269N mutants was significantly lower than that of the H269C mutant. Site-directed mutagenesis of Asp-320 to asparagine produced an insoluble protein, whereas mutation to alanine and cysteine resulted in soluble protein with undetectable catalytic activity. However, these two mutants were still able to bind a significant amount of zinc. The mutation of Glu-235 was less disruptive than the modifications to either His-269 or Asp-320. Reductions of 2−4 orders of magnitude were found for k_{cat} and k_{cat}/K_m relative to the wild type enzyme. However, the Michaelis constants were in an experimentally accessible range.

pH−Rate Profiles. The kinetic constants for the enzymatic hydrolysis of *N*-formimino-L-glutamate by HutF were determined as a function of pH. The plots of k_{cat} and k_{cat}/K_m versus pH for the zinc substituted enzyme are presented in Figure 2. The shape of these two pH−rate profiles indicates that two groups are required to be in the proper state of ionization for maximum catalytic activity; one of these groups must be ionized while the other must be protonated. When the native zinc in the active site is replaced with other
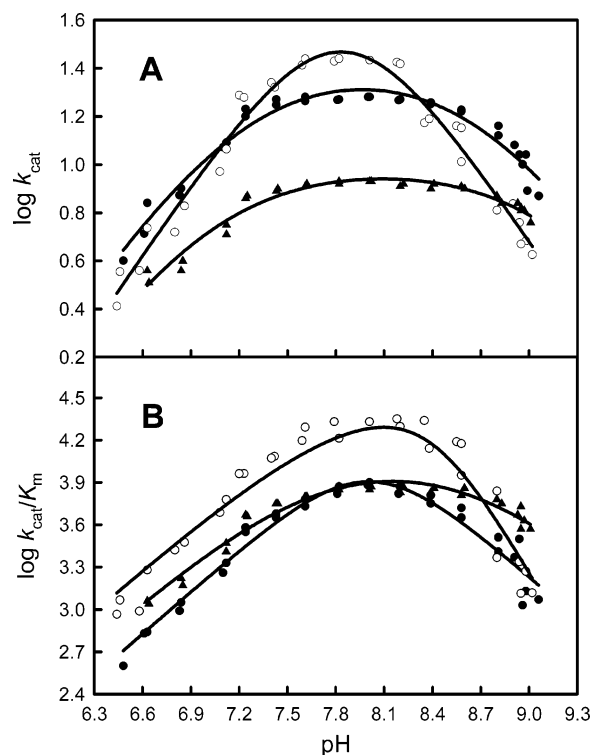
Table 2: Ionization Constants for Metal-Substituted HutF from pH−Rate Profiles[a]

HutF	log k_{cat} vs pH		log k_{cat}/K_m vs pH	
	pK_a	pK_b	pK_a	pK_b
WT (Zn)	7.1 ± 0.2	8.2 ± 0.2	7.3 ± 0.1	8.5 ± 0.1
WT (Ni)	7.2 ± 0.1	8.7 ± 0.1	8.1 ± 0.1	8.1 ± 0.1
WT (Cd)	7.8 ± 0.1	7.8 ± 0.1	7.7 ± 0.3[b]	8.7 ± 0.2[b]
WT (Cu)	7.0 ± 0.1	8.8 ± 0.2	7.5 ± 0.3	8.8 ± 0.3
E235Q (Zn)	7.3 ± 0.4	8.6 ± 0.2	7.1 ± 0.4[c]	>9.2[c]
E235A (Zn)	7.4 ± 0.1	9.1 ± 0.1	7.5 ± 0.6[c]	8.9 ± 0.1[c]

[a] The kinetic constants were determined using *N*-formimino-L-glutamate as the substrate from fits of the data to eq 2. [b] Values obtained from fits of the data to eq 3. [c] Values were obtained from fits of the data to eq 4.

divalent cations, the pK values for the groups that ionize within this pH range change slightly (Figure 3). For Cd-HutF, the two ionizations are very close to one another in the pH−rate profile of k_{cat}, and it is not possible to accurately obtain the values for pK_a and pK_b when the difference between them is less than 0.6 pK units (*7*). The fitting routine therefore assumes that the two ionizations have the same pK value (*7*). A similar situation applies to the pH rate profile of k_{cat}/K_m for Ni-HutF. For Cd-HutF, the pH−rate profile for k_{cat}/K_m decreases with a slope of −2 for the group(s) that must be protonated for activity. These data were fit to eq 3, which assumes that both ionizations have the same value for pK_b. The pK values from the kinetic measurements are presented in Table 2.

The pH−rate profiles were determined for the E235Q and E235A mutants. The pH−rate profiles for k_{cat} are bell-shaped with activity decreasing at high and low values of pH. For
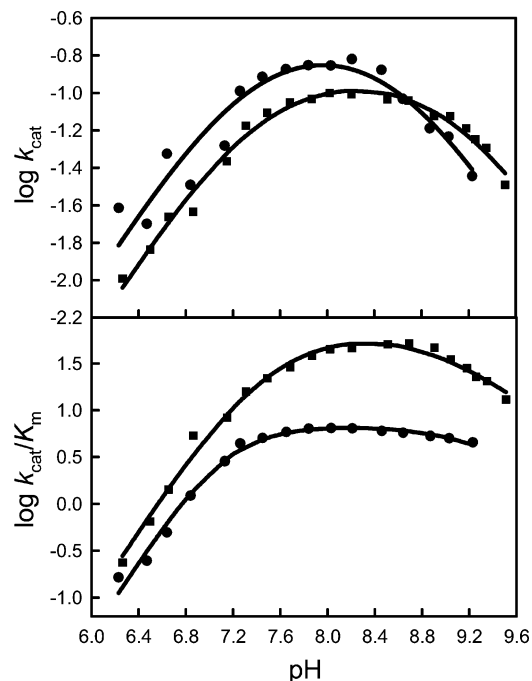
FIGURE 4: pH–rate profiles of k_{cat} and k_{cat}/K_m for the zinc substituted forms of the mutants E235A (●) and E235Q (■). The data were fit to eq 4. Additional details are provided in the text and in Table 2.

k_{cat}/K_m the activity is lost at low pH with a slope of 2 indicating the protonation of two residues. In addition, the pK for the group that ionizes at high pH for the E235Q mutant is higher relative to the wild type enzyme (>9.2 vs 8.5). The pH–rate profiles for the E235Q and E235A mutants are presented in Figure 4, and the pK values from fits of the data to eqs 2 or 4 are provided in Table 2.

DISCUSSION

A number of enzymes within the amidohydrolase super-family catalyze the deamination of purine and pyrimidine nucleotides, including cytosine, adenosine, and guanine deaminase. All of these nucleotides contain structural motifs that are homologous to the formimino substituent in *N*-formimino-L-glutamate. The chemical reaction mechanism for adenosine deaminase has been elaborated through a comprehensive array of biochemical, computational, and crystallographic experiments (*8*, *10*–*13*). In these investigations several residues within the active site of ADA have been recognized to be directly involved in substrate binding and catalysis. The most salient residues for adenosine deaminase from mouse include Glu-217, His-238, and Asp-295. A homologous trio of amino acids is predicted to function in an analogous fashion in cytosine deaminase (*9*), guanine deaminase (*5*), and AMP deaminase (*5*). In these enzymes a water molecule is coordinated to the single divalent cation localized to the M_α-position in the active site. The water molecule is furthered hydrogen bonded to a histidine from strand 6 and an aspartate from strand 8. The glutamic acid from strand 5 functions as a general acid through proton transfer to the aromatic leaving group. Although HutF does not catalyze the deamination of an aromatic amine, it does catalyze the analogous deimination of an *N*-formimino group to an *N*-formamide derivative.

A working model for the chemical mechanism of the reaction catalyzed by HutF is presented in Scheme 3. In this mechanism the single divalent cation is bound to His-56 and His-58 from strand 1, His-232 from strand 5, and Asp-320 from strand 8. The final ligand to this metal ion is a water molecule that is in turn hydrogen bonded to His-269 from strand 6 and Asp-320 from strand 8 (see also Figure 1). The substrate binds into the active site in an orientation such that the metal bound water molecule is poised to attack the formimino functional group. The pK_a value of the formimino group is approximately 11.2 (*16*), and thus the substrate likely binds with the *N*-formimino group protonated, but it is unclear as to the relative distribution of the positive charge over the two nitrogen atoms. Once bound, the side chain carboxylate of Glu-235 makes an electrostatic interaction with the positively charged formimino group of the substrate. In this proposed mechanism the reaction is initiated by the abstraction of a proton from the bound water molecule by the side chain imidazole of His-269 to generate a tetrahedral intermediate. The collapse of the tetrahedral intermediate commences with the abstraction of the second proton via the side chain carboxylate of Asp-320. The C–N bond is then cleaved concomitantly with proton transfer from His-269 to liberate ammonia and generate the *N*-formyl product. After product release the resting state of the enzyme is regenerated after the binding of another water molecule.

A single divalent metal ion is essential for the catalytic activity of HutF. The most active enzyme was found to contain one equivalent of Zn per protein subunit. The metal ion can be removed by metal chelators, and the apoenzyme is essentially inactive. The apoenzyme can be reconstituted with one equivalent of Zn, Cd, Ni, or Cu with a modest variation in the final catalytic activity. It is assumed that Zn is the native divalent cation. The loss of activity after removal of the divalent cation from the active site of HutF is consistent with the role of the metal ion as a binding site for the nucleophilic water molecule. Similar results have been found for other members of the amidohydrolase superfamily (*8*, *9*, *14*, *15*). The loss of activity exhibited by HutF at low pH for the Zn²⁺-substituted enzyme indicates the protonation of a single group with a pK_a of approximately 7.3. Since the substrate does not ionize at this pH (*16*), it is assumed that this ionization must originate with the enzyme. Therefore, the most likely candidate for the group that must be deprotonated for catalytic activity is the histidine from strand 6 (His-269) that is hydrogen bonded to the water molecule that is ligated to the lone divalent cation in the active site. This conclusion is supported by the catastrophic loss of activity when this residue is mutated to alanine, cysteine, or asparagine. It should be noted, however, that the H269A and H269N mutants have a somewhat lower metal occupancy than the wild type HutF.

Activity is also lost at high pH when a functional group is deprotonated. The decrease in catalytic activity at high pH for the k_{cat}/K_m profile suggests the deprotonation of a group with a pK value of around 8.5. Based on the crystal structures of cytosine deaminase (*9*) and adenosine deaminase (*8*, *13*) and the comparison of their amino acid sequences with the amino acid sequence of HutF, there is no obvious residue within the active site of HutF that might be responsible for the decrease in activity at high pH. The pK_a value for the formimino group of *N*-formimino-L-glutamate has been reported to be 11.2 (*16*), and thus the ionization of the substrate does not appear to be responsible for the

Scheme 3
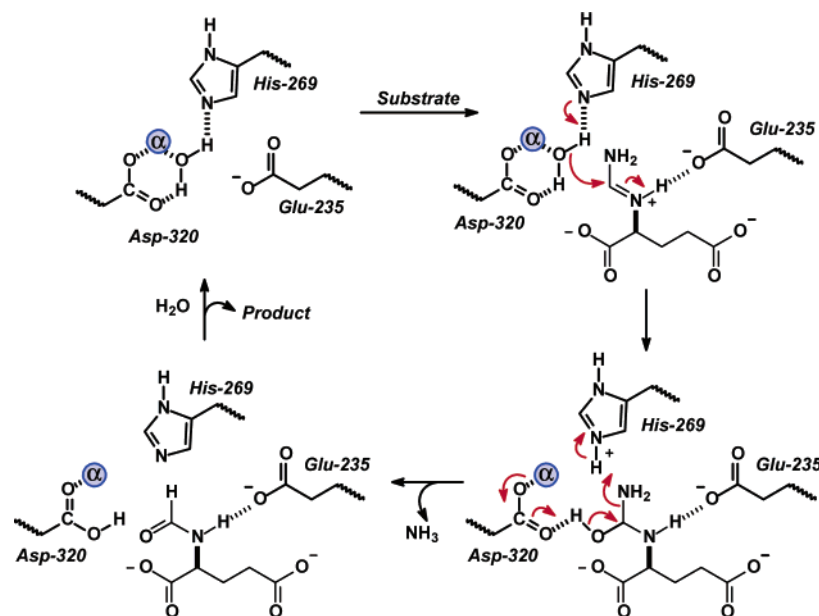
diminution of catalytic activity at high pH. It is unclear as to the group that is responsible for the loss of activity at high pH.

In the mechanism proposed in Scheme 3 the other residue that serves to activate the water in conjunction with His-269 is Asp-320 from strand 8. When this residue is mutated to either alanine or cysteine, the catalytic activity of HutF is reduced by over 6 orders of magnitude. Even though this residue also ligates to the divalent cation in the active site, these two mutants are still able to bind a significant amount of zinc. The substantial loss of catalytic activity is consistent with the role proposed by this residue during the deimination of the substrate.

In the mechanisms of action proposed for the deamination of adenosine and cytosine, the invariant glutamate in the HxxE motif at the end of strand 5 serves to donate a proton to the ring nitrogen during the course of the reaction. In the reaction catalyzed by HutF, the role of this highly conserved residue must be slightly different. Since the formimino group of the substrate is protonated, there is no reason why this residue must function as a general acid. It can, however, function as an electrostatic bridge from the protein to the substrate. The importance of this interaction is reflected in the loss of activity when this residue (E235) is mutated to either alanine, aspartate, or glutamine. The E235A mutant is the most active of the three modifications made to this site, but it is reduced in catalytic activity by 3 orders of magnitude. The lost of the negative charge for the mutants E235A and E235Q has increased the K_m for the substrate by a factor of 10 and 88, respectively. The pH−rate profiles for the E235Q and E235A mutants are similar to the wild type Zn-HutF. However, in the pH−rate profile for k_{cat}/K_m, the loss in activity at low pH is more pronounced in that the data are best fit to the protonation of two groups at low pH with an average pK_a of about 7.3. The exact reason for this difference in the pH−rate profiles is not known, but one possibility is that in these mutants we are observing the protonation of both His-269 and Asp-320. Regardless, the substantial loss of activity upon the mutation of Glu-235 is consistent with the proposed role that this residue plays in

the deimination of *N*-formimino-L-glutamate. An alternate function for Glu-235 is the abstraction of the proton from the tetrahedral intermediate instead of Asp-320 as suggested in Scheme 3.

Summary. HutF is a newly identified member of the amidohydrolase superfamily that catalyzes the deimination of *N*-formimino-L-glutamate (*2*). Sequence comparisons with other members of this superfamily indicate that the active site most closely resembles those enzymes that catalyze the deamination of aromatic bases such as adenine, guanine, and cytosine (*2*). Mutagenesis of three key residues (Glu-235, His-269, and Asp-320) has enabled a reaction mechanism to be proposed for the deimination of *N*-formimino-L-glutamate that is very similar to the mechanisms required for the deamination of adenine, guanine, and cytosine.

ACKNOWLEDGMENT

REFERENCES

1. Borek, B. A., and Waelsch, H. (1953) The enzymatic degradation of histidine, *J. Biol. Chem. 205*, 459−474.
2. Marti-Arbona, R., Xu, C., Steele, S., Weeks, A., Kuty, G. F., Seibert, C. M., and Raushel, F. M. (2006) Annotating enzymes of unknown function: *N*-formimino-L-glutamate deiminase is a member of the amidohydrolase superfamily, *Biochemistry 45*, 1997−2005.
3. Holm, L., and Sander, C. (1997) An evolutionary treasure: Unification of a broad set of amidohydrolases related to urease, *Proteins 28*, 72−82.
4. Roodveldt, C., and Tawfik, D. S. (2005) Shared promiscuous activities and evolutionary features in various members of the amidohydrolase superfamily, *Biochemistry 44*, 12728−12736.
5. Seibert, C. M., and Raushel, F. M. (2005) Structural and catalytic diversity within the amidohydrolase superfamily, *Biochemistry 44*, 6383−6391.
6. Muszbek, L., Polgar, J., and Fesus, L. (1985) Kinetic determination of blood coagulation factor xiii in plasma, *Clin. Chem. 31*, 35−40.
7. Cleland, W. W. (1979) Statistical analysis of enzyme kinetic data, *Methods Enzymol. 63*, 103−138.

8. Wang, Z., and Quiocho, F. A. (1998) Complexes of adenosine deaminase with two potent inhibitors: X-ray structures in four independent molecules at pH of maximum activity, *Biochemistry 37*, 8314−8324.

9. Ireton, G. C., McDermott, G., Black, M. E., and Stoddard, B. L. (2002) The structure of *Escherichia coli* cytosine deaminase, *J. Mol. Biol. 315*, 687−697.

10. Kurz, L. C., Moix, L., Riley, M. C., and Frieden, C. (1992) The rate of formation of transition-state analogues in the active site of adenosine deaminase is encounter-controlled: Implications for the mechanism, *Biochemistry 31*, 39−48.

11. Kinoshita, T., Nakanishi, I., Terasaka, T., Kuno, M., Seki, N., Warizaya, M., Matsumura, H., Inoue, T., Takano, K., Adachi, H., Mori, Y., and Fujii, T. (2005) Structural basis of compound recognition by adenosine deaminase, *Biochemistry 44*, 10562−10569.

12. Frick, L., Wolfenden, R., Smal, E., and Baker, D. C. (1986) Transition-state stabilization by adenosine deaminase: Structural studies of its inhibitory complex with deoxycoformycin, *Biochemistry 25*, 1616−1621.

13. Wilson, D. K., and Quiocho, F. A. (1993) A pre-transition-state mimic of an enzyme: X-ray structure of adenosine deaminase with bound L-deazaadenosine and zinc-activated water, *Biochemistry 32*, 1689−1694.

14. Babbitt, P. C., Mrachko, G. T., Hasson, M. S., Huisman, G. W., Kolter, R., Ringe, D., Petsko, G. A., Kenyon, G. L., and Gerlt, J. A. (1995) A functionally diverse enzyme superfamily that abstracts the alpha protons of carboxylic acids, *Science 267*, 1159−1161.

15. Seffernick, J. L., McTavish, H., Osborne, J. P., de Souza, M. L., Sadowsky, M. J., and Wackett, L. P. (2002) Atrazine chlorohydrolase from *Pseudomonas* sp. strain ADP is a metalloenzyme, *Biochemistry 41*, 14430−14437.

16. Tabor, H., and Mehler, A. H. (1954) Isolation of *N*-formyl-L-glutamic acid as an intermediate in the enzymatic degradation of L-histidine, *J. Biol. Chem. 210*, 559−568.